Review of Scientific Instruments

Measurements of radial profile of hydrogen and deuterium density in isotope mixture plasmas using bulk charge exchange spectroscopy

Cite as: Rev. Sci. Instrum. **90**, 093503 (2019); https://doi.org/10.1063/1.5097030
Submitted: 22 March 2019 • Accepted: 17 August 2019 • Published Online: 06 September 2019

K. Ida, M. Yoshinuma, K. Yamasaki, et al.

Review of Scientific Instruments ARTICLE scitation.org/journal/rsi

Measurements of radial profile of hydrogen and deuterium density in isotope mixture plasmas using bulk charge exchange spectroscopy

Cite as: Rev. Sci. Instrum. 90, 093503 (2019); doi: 10.1063/1.5097030
Submitted: 22 March 2019 • Accepted: 17 August 2019 •
Published Online: 6 September 2019

K. Ida,[1,2,a] M. Yoshinuma,[1,2] K. Yamasaki,[3] T. Kobayashi,[1,2] Y. Fujiwara,[1] J. Chen,[4] I. Murakami,[1,2] S. Satake,[1,2] Y. Yamamoto,[5] S. Murakami,[5] and M. Kobayashi[1,2]

AFFILIATIONS

[1]National Institute for Fusion Science, National Institutes of Natural Sciences, Toki, Gifu 509-5292, Japan
[2]SOKENDAI (The Graduate University for Advanced Studies), Toki, Gifu 509-5292, Japan
[3]Research Institute for Applied Mechanics Kyushu University, Kasuga, Fukuoka, Japan
[4]School of Nuclear Science and Technology, University of Science and Technology of China, Hefei 230026, China
[5]Department of Nuclear Engineering, Kyoto University, Kyoto 615-8450, Japan

[a]**Electronic mail:** ida@nifs.ac.jp

ABSTRACT

A bulk charge exchange spectroscopy system has been applied to measure the radial profiles of the hydrogen (H) and deuterium (D) density ratio in the isotope mixture plasma in a large helical device. Charge exchange lines of H_α and D_α are fitted by 4 Gaussian of H and D cold components and H and D hot components with 5 parameters by combining the measurement of plasma toroidal rotation velocity with carbon charge exchange spectroscopy. The radial profiles of the relative density of hydrogen and deuterium ions are derived from H and D hot components measured and the beam density calculated from beam attenuation calculation. A proof-of-principle experiment is performed by the H pellet and the D pellet injections into the H-D mixture plasma.

I. INTRODUCTION

The isotope effect of ion particle transport is a very important issue in the fusion plasmas where the control of isotope ratio in the core plasma is indispensable for optimizing the fusion output due to the deuterium-tritium (D-T) reaction. The isotope effect of ion particle transport cannot be directly observed in pure hydrogen (H) or pure deuterium (D) because of the degeneration between ion particle transport and electron particle transport due to the quasineutralization condition. Therefore, the transport study in the D-H mixture plasma is essential for decoupling the ion particle transport and the electron particle transport. Recently, the difference in H ion transport and D ion transport in the D-H mixture plasma becomes an important topic for understanding the isotope difference in the ion transport and predicting the D-H ratio or the D-T ratio in the plasma.

The first measurements of the transport coefficient of the hydrogen isotope in tokamak plasma were performed in TFTR.[1] Tritium density is inferred from the time evolution of the neutron emissivity profiles, and transport coefficients (D, V) are determined by puffing a small amount of tritium (T) gas into deuterium plasmas. More recently, deuterium and hydrogen densities were measured in the D-H mixture plasma with a recycling particle source of H and D.[2] In these experiments, the central deuterium density and, hence, the D-H ratio at the plasma center are evaluated from the neutron rate, while the D-H ratio at the plasma edge is evaluated from the H_α and D_α line ratio measured with passive spectroscopy. D-H ratio profiles are found to

be insensitive to the isotope species of the recycling from the wall in JET.

Despite the importance of understanding the isotope difference in ion particle transport in the isotope mixture plasma, where the ion particle transport is decoupled from the electron particle transport, there are only few results reported due to the lack of precise measurement of the D-H ratio in the plasma core. In order to understand the ion particle transport in the isotope mixture plasma, a novel diagnostic technique to measure the D-H density ratio is necessary. In this paper, the measurements of the D-H density ratio using bulk charge exchange spectroscopy combined with the measurement of carbon charge exchange spectroscopy[3] are described.

II. EXPERIMENTAL SETUP

In order to develop the isotope ratio measurements in the plasma core, a bulk charge exchange spectroscopy system has been installed in a Large Helical Device (LHD). The bulk charge exchange system consists of a 300 mm F2.8 camera lens, 2160/mm diffraction grating, and CCD detector (Andor DU897D 16 × 16 μm^2 512 × 512 pixels). The dispersion is 0.72 nm/mm at 656 nm. 32 optical fibers with a diameter of 200 μm are arranged at the entrance slit of the spectrometer, which provides 32 channels. The time resolution is determined by the integration time of the CCD detector and is typically 5 ms. The radial profiles of hydrogen fraction $n_H/(n_H + n_D)$ or deuterium fraction $n_D/(n_H + n_D)$ in the plasma can be measured from the H_α and D_α lines emitted by the charge exchange reaction between the bulk ions and the neutral beam injected. Usually, bulk charge exchange spectroscopy has been used to measure the toroidal rotation velocity in the hydrogen or deuterium plasma where the fraction of hydrogen and deuterium is close to unity and relatively constant in space.[4,5] In the LHD, bulk charge exchange spectroscopy[6–8] has been applied for the measurement of the radial profiles of the D-H density ratio[9] in the D-H mixture plasma to study the isotope effect of ion particle transport.

Figure 1 shows the geometry of the line of sight, beam line, and toroidal direction in the experimental setup of the LHD. The

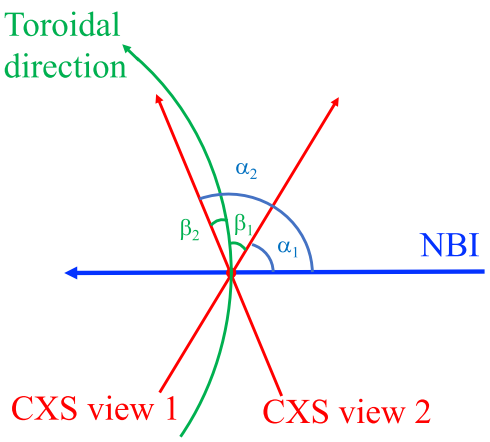

FIG. 1. Experimental setup: geometry of neutral beam and the line of sight of bulk charge exchange spectroscopy.

α is the angle between the line of sight and the beam line, while the β is the angle between the line of sight and the toroidal direction. In order to separate the beam emission line and the charge exchange line, α should be small. However, the larger α is preferable for minimizing the error due to the uncertainty of energy dependence of the emission cross section.[10] In contrast, smaller β is better to measure the plasma flow parallel to the magnetic flux surface, where the difference between the impurity flow and the bulk flow is relatively small compared with the flow perpendicular to the magnetic flux surface. Then, the optimum of the angle between the line of sight and the beam line α_1 is 60° and α_2 is 120°, while the optimum of the angle between the line of sight and the toroidal direction is $\beta_1 = -30°$ and $\beta_2 = 30°$. In the experimental setup in the LHD, $\alpha_1 = 61°$, $\alpha_2 = 103°$, $\beta_1 = -29°$, and $\beta_2 = 13°$. The angles of view 1 are close to the optimized value, while the angles of view 2 are too perpendicular to the beam line. The Doppler broadening of H_α is 1.4 times larger than that of D_α for the equal temperature between hydrogen and deuterium. The blue wing of the charge exchange line is mainly provided by the blue wing of D_α (656.1 nm), while the red wing of the charge exchange line is mainly contributed by the red wing of H_α (656.28 nm). Therefore, the height of the wing of the charge exchange spectra becomes asymmetric (the red wing of the spectrum is higher than the blue wing) even for the n_H:n_D = 1:1 mixture plasma without toroidal rotation. Therefore, the line of sight antiparallel to the neutral beam line, in which the beam emission is in the blue shift, is preferable for avoiding the overlapping between the red wing and the beam emission.

The toroidal rotation velocity of carbon impurity, V_ϕ^C, is derived from the Doppler shift of carbon line, λ_s^C, with the velocity correction due to the energy-dependent charge exchange cross section of carbon line, V_{cor}^C, as

$$V_\phi^C = c(\lambda_s^C/\lambda_0^C)/\cos\beta - \mathrm{V}_{\mathrm{cor}}^{\mathrm{C}}\cos\alpha/\cos\beta, \quad (1)$$

where λ_0^C is the wavelength of carbon line and c is the velocity of light. The toroidal rotation velocities of hydrogen and deuterium, V_ϕ^H and V_ϕ^D, are derived from the measured toroidal rotation velocity of carbon impurity, V_ϕ^C, and velocity differences between hydrogen or deuterium bulk ions and carbon impurity ion calculated, δV_ϕ^{H-C} or δV_ϕ^{D-C}, respectively,

$$V_\phi^H = V_\phi^C + \delta V_\phi^{H-C}, \quad (2)$$

$$V_\phi^D = V_\phi^C + \delta V_\phi^{D-C}. \quad (3)$$

The Doppler shifts of hydrogen and deuterium, λ_s^H and λ_s^D, are derived from the toroidal rotation velocity of hydrogen and deuterium, V_ϕ^H and V_ϕ^D, with the corrections due to the energy dependent emission cross section of hydrogen and deuterium lines, V_{cor}^H and V_{cor}^D, as

$$c(\lambda_s^H/\lambda_0^H) = V_\phi^H\cos\beta + \mathrm{V}_{\mathrm{cor}}^{\mathrm{H}}\cos\alpha, \quad (4)$$

$$c(\lambda_s^D/\lambda_0^D) = V_\phi^D\cos\beta + \mathrm{V}_{\mathrm{cor}}^{\mathrm{D}}\cos\alpha, \quad (5)$$

where λ_0^H and λ_0^D are the wavelengths of Hα and Dα lines, respectively.

III. SPECTRUM OF Hα AND Dα MEASURED WITH BULK CHARGE EXCHANGE SPECTROSCOPY

The hot component due to the active charge exchange reaction with the neutral beam is smaller than the cold component emitted in the edge by one order of magnitude. In order to subtract the cold component of the H_α and D_α charge exchange lines, the beam modulation technique is applied. Figure 2 shows the spectra of H_α and D_α lines at beam-on and beam-off timing and the differences in these two time slices after subtracting the spectrum at beam-off timing from the spectrum at beam-on timing for the discharge with D-H mixture plasmas. Although most of the cold components of the charge exchange lines are subtracted by the beam modulation, there still remain cold components (residual cold component) comparable to the hot components as seen in the spectrum after subtraction in the bulk charge exchange lines. There are small wings of the spectra in the plasma even without beam due to the charge exchange process between the thermal neutral penetrated into the plasma and bulk ions. This is called the passive charge exchange or medium temperature component,[11] and most of the medium temperature components can be subtracted by the beam modulation technique. In the LHD, the radial profile of neutral is measured from this passive charge exchange component using the spectrometer with a high dynamic range.[12] The passive charge exchange component is smaller than the cold component by two orders of magnitude (smaller than the active charge exchange component excited by neutral beam by a factor of 5–10). The residual passive charge exchange component is expected to be smaller than the residual cold component by two orders of magnitude (below the noise level) and can be neglected.

Because of the residual cold component, the slit width of the spectrometer is reduced to 50 μ to make the instrumental width (FWHM) small enough (0.056 nm) to separate the two peaks of the cold components of H_α (656.28 nm) and D_α (656.10 nm) lines in the spectrum. The Doppler width of the cold component is smaller than the wavelength separation (0.18 nm) between the H_α and D_α lines, while the Doppler width of the hot component is too large to be separated into two peaks. The lines in the wavelength range of 653–655 nm are beam emissions of hydrogen beam with full, half, and one-third energy. As discussed in Sec. II, the line of sight is selected to make the beam emission blue shift to have more separation between beam emission lines and the charge exchange line.

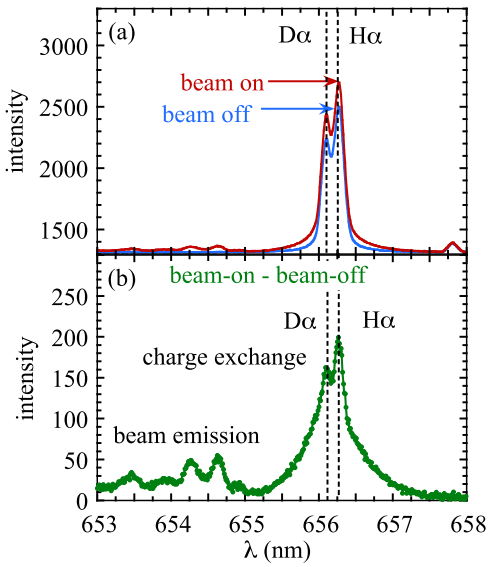

FIG. 2. Hα and Dα spectrum at (a) beam-on and beam-off timing and (b) the difference of the spectrum between beam-on and beam-off timing.

IV. ANALYSIS METHOD FOR HYDROGEN AND DEUTERIUM DENSITY PROFILE MEASUREMENT

A. Fitting of spectrum with four Gaussian

Figure 3 shows H_α and D_α spectra before pellet injection, after deuterium pellet injection, and after hydrogen pellet injection. The most significant differences between these two spectra appear at the red wing of the spectrum. This is because both the red shift and the wider Doppler shift of H hot component contribute to the increase of the red wing, while their effects cancel each other in the blue wing. Charge exchange lines are fitted by four Gaussian of H

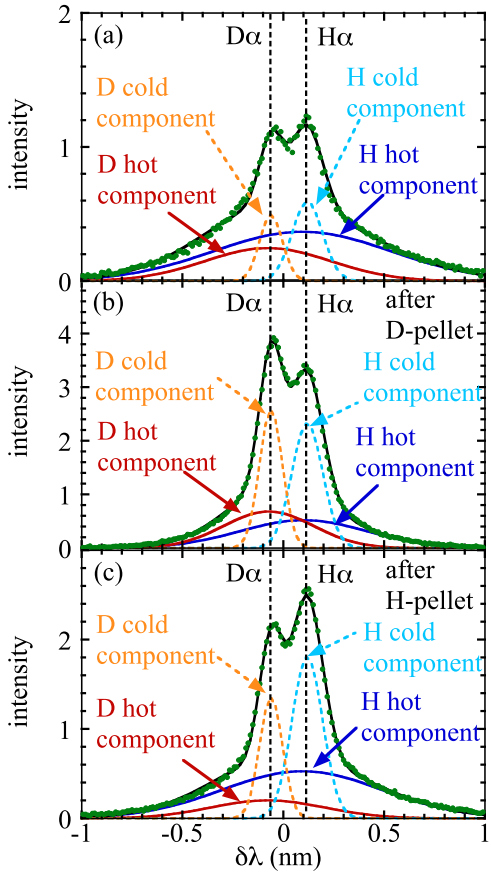

FIG. 3. Hα and Dα spectrum: (a) before pellet injection, (b) after deuterium pellet injection, and (c) after hydrogen pellet injection.

and D cold components and H and D hot components,

$$I(\lambda) = \sum_{i}^{4}\left[A^{i}\exp\left(-\frac{(\lambda-\lambda_0^i-\lambda_s^i)^2}{(\lambda_w^i)^2+(\lambda_{\rm ins})^2}\right)\right]. \quad (6)$$

There are 3 parameters (amplitude A^i, Doppler shift λ_s^i, and $1/e$ Doppler width λ_w^i) for each Gaussian profile, and the total number of parameters for four Gaussian profiles is 12. Here, i denotes the H and D hot and cold components as i = Hcold, Hhot, Dcold, and Dhot. λ_0^i is the wavelength with no Doppler shift, and $\lambda_{\rm ins}$ is the instrumental width of the spectrometer for the 50 μ slit width ($\lambda_0^{\rm Hcold} = \lambda_0^{\rm Hhot} = 656.28$ nm, $\lambda_0^{\rm Dcold} = \lambda_0^{\rm Dhot} = 656.1$ nm, and $\lambda_{\rm ins} = 0.04$ nm). In order to reduce the number of free parameters, the Doppler width and the shift of H and D cold components ($\lambda_w^{\rm Hcold}$, $\lambda_s^{\rm Hcold}$, $\lambda_w^{\rm Dcold}$, and $\lambda_s^{\rm Dcold}$) are given by fitting the spectrum at beam-off timing with the assumption of $T_i^{\rm Hcold} = T_i^{\rm Dcold}$. Doppler widths of the H and D hot components ($\lambda_w^{\rm Hhot}$ and $\lambda_w^{\rm Dhot}$) are given by the fitting of the spectrum after the subtraction with the assumption of equal ion temperature between hydrogen and deuterium ($T_i^{\rm Hhot} = T_i^{\rm Dhot}$).

The Doppler shift of the H and D hot components ($\lambda_s^{\rm Hhot}$, $\lambda_s^{\rm Dhot}$) is given by the toroidal carbon flow velocity with the velocity correction due to the energy-dependent charge exchange cross section. Here, the velocity differences between carbon and bulk ion are ignored because the difference is small enough to be neglected, as discussed in Sec. IV C. Then, the following five free parameters for the spectrum fitting are selected: the amplitude of cold and hot components of hydrogen and deuterium and ion temperature of bulk ions ($A^{\rm Hcold}$, $A^{\rm Hhot}$, $A^{\rm Dcold}$, $A^{\rm Dhot}$, and $\lambda_w^{\rm Hhot}[216\,000 = \sqrt{2}\lambda_w^{\rm Dhot}]$). Although both hot and cold components of hydrogen (deuterium) increase after the hydrogen (deuterium) pellet, the increase of the hot component is much more significant. This is explained by the fact that the increase of the hot component is due to the increase of the density, while the increase of the cold component is due to the increase of recycling after the pellet injection.

B. Correction of toroidal velocity measurements

It is well known that the rotation velocity measured with charge exchange spectroscopy requires a correction due to the energy dependent cross section because the wavelength shift appears in the charge exchange line when $(1/Q)\partial Q/\partial V$ is finite.[13,14] Here, Q is the emission cross section for the transition observed in the charge exchange spectroscopy and V is the velocity of the probe neutral beam. The correction velocity $V_{\rm cor}$ is roughly proportional to ion temperature and in the direction of the upstream of the neutral beam for $(1/Q)\partial Q/\partial V > 0$ and toward the downstream of the neutral beam for $(1/Q)\partial Q/\partial V < 0$. Although the correction velocity normalized by ion temperature can be evaluated by the Atomic Data and Analysis Structure (ADAS),[15] the fraction of $n = 2$ excited state should be determined experimentally because the contribution of the $n = 2$ excited state donor to effective emission is significant at lower beam energy and has a significant influence on the values of $(1/Q)\partial Q/\partial V$ at the beam energy below 35 keV/amu especially for the charge exchange lines of carbon. In the LHD, $V_{\rm cor}/T_i$ is experimentally determined by measuring the ion temperature dependence of wavelength shift of charge exchange line along the beam line. The $(1/Q)\partial Q/\partial V$ evaluated from the $V_{\rm cor}/T_i$ measured shows the best fit to the $(1/Q)\partial Q/\partial V$ evaluated from ADAS with the fraction of $n = 2$ excited state of 0.2%.

Figure 4 shows the correction coefficient of toroidal velocity due to the cross-sectional effect for carbon, hydrogen, and deuterium as a function of beam energy per atomic unit for the $n = 2$ excited states of 0.2%.[16] In the case of the hydrogen beam where the energy range of 30–50 keV/amu, wavelength shift due to the energy dependent charge exchange cross section is toward the upstream of the neutral beam for carbon and toward the downstream of the neutral beam for hydrogen and deuterium. However, in the case of the deuterium beam where the energy range of 20–30 keV/amu, wavelength shift due to the energy dependent charge exchange cross section is toward the upstream of the neutral beam for both carbon and bulk ions. Because the velocity correction is roughly proportional to the ion temperature, precise evaluation of $(1/Q)\partial Q/\partial V$ becomes more important at higher ion temperature. If the line of sight of the measurement is perpendicular to the beam line, the wavelength shift due to the energy dependent emission cross section can be minimized. However, in order to separate the charge exchange emission and beam emission, the line of sight should be tilted from the perpendicular direction of the neutral beam, and the optimum tilted angle to the beam line is 60° in the LHD.

Figure 5 shows the radial profile of ion temperature of carbon and atomic correction of toroidal rotation for carbon ion and hydrogen and deuterium ions for the hydrogen beam with the beam energy of 43 keV/amu.[16] It should be noted that the correction of the velocity plotted in Fig. 5 is along the toroidal direction and not along the beam line and also not along the line of sight. Here, positive velocity is a red shift due to the counterclockwise (CCW) toroidal rotation and negative velocity is a blue shift due to the CW toroidal rotation, as seen in Fig. 1. The velocity correction is 13 km/s in CW direction for carbon and 17 km/s and 28 km/s in CCW direction for deuterium and hydrogen ions, respectively. In order to measure

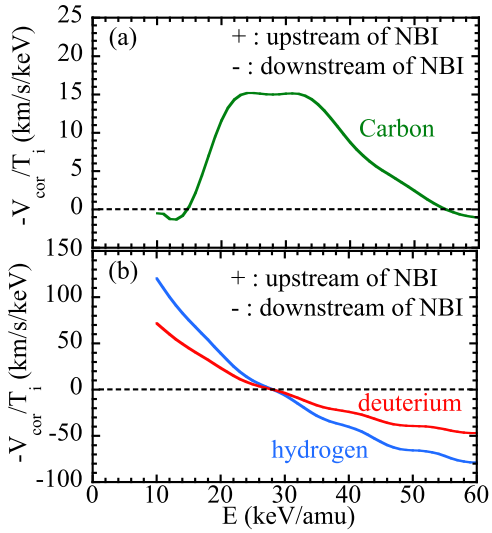

FIG. 4. Correction coefficient of toroidal velocity due to cross-sectional effect on (a) carbon and (b) hydrogen and deuterium as a function of beam energy per atomic unit. Here, the fraction of $n = 2$ excited state is 0.2%.

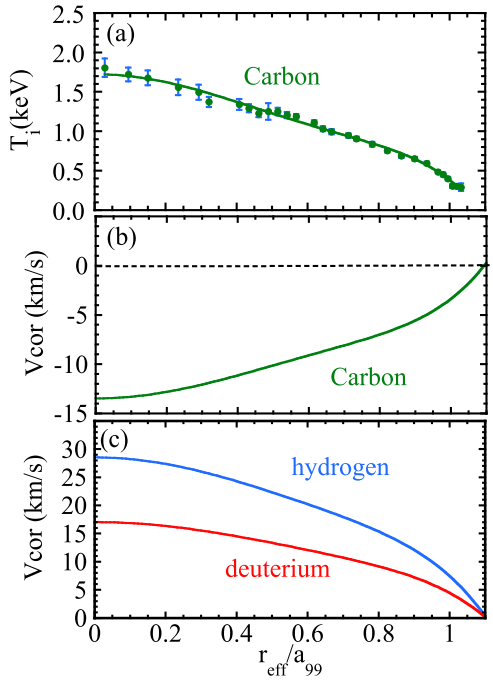

FIG. 5. Radial profile of (a) ion temperature of carbon and atomic correction of toroidal rotation for (b) carbon ion and (c) hydrogen and deuterium ions. Here, positive velocity is a red shift and negative velocity is a blue shift. Here, the beam species is hydrogen and beam energy is 43 keV/amu.

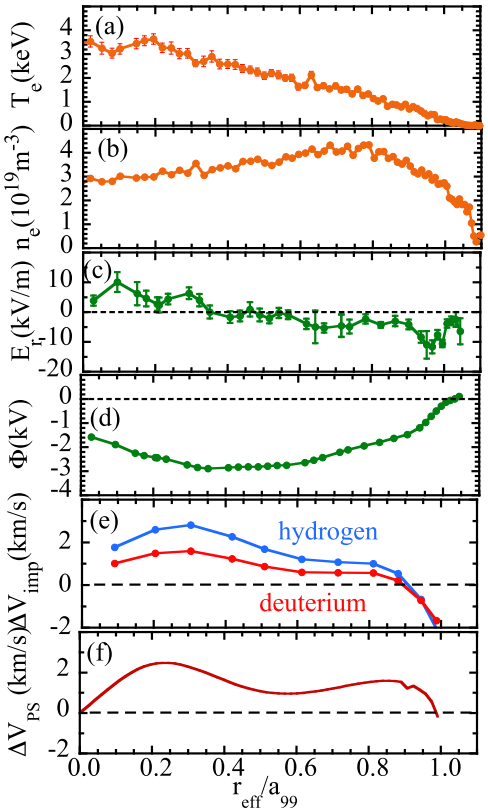

FIG. 6. Radial profile of (a) electron temperature, (b) electron density, (c) radial electric field, (d) space potential, (e) velocity differences between hydrogen or deuterium bulk ions and the carbon impurity ion calculated by the DKES code, and (f) velocity difference of Pfirsch-Schlüter flow between bulk ions and the carbon impurity ion calculated. Here, positive velocity is in codirection and negative velocity is in the counter-direction.

the D-H ratio precisely, the accurate evaluation of energy dependent emission cross-sectional effect is essential.

C. Velocity difference between carbon impurity and bulk ions

In general, the flow velocity parallel to the magnetic field of impurity is not equal to that of bulk ions. In the LHD, the differences of flux averaged parallel flow between impurity and bulk ions ΔV_{imp} are evaluated with neoclassical calculation using the Drift Kinetic Equation Solver (DKES) code,[17–19] while the differences of Pfirsch-Schlüter flow ΔV_{PS} between impurity and bulk ions are evaluated by the geometric factor[20,21] with incompressibility conditions of parallel flow.[22–24] These flows are calculated from the magnetic field structure with finite pressure and measured radial profiles of pressure and space potential. Figure 6 shows the radial profile of electron temperature, electron density, radial electric field, and space potential. The velocity differences between hydrogen or deuterium bulk ions and the carbon impurity ion calculated by the DKES code are shown in Fig. 6(c). The velocity differences of Pfirsch-Schlüter flow between bulk ions and the carbon impurity ion calculated are also plotted. Here, positive velocity is in codirection and negative velocity is in counter-direction. The central electron temperature and the ion temperature are 3 keV and 2 keV, respectively, while the central electron density is 3×10^{19} m^{-3}. The radial electric field is slightly positive in the core and slightly negative near the plasma periphery. As seen in Fig. 6(e), the velocity differences of flux averaged parallel flow between hydrogen or deuterium bulk ions are only 2–3 km/s and much smaller than the velocity correction. The velocity differences of Pfirsch-Schlüter flow between bulk ions are also only 2–3 km/s. (The velocity difference is identical to hydrogen and deuterium ions.) The wavelength separation between Hα and Dα is 0.18 nm and corresponds to the Doppler shift of bulk ions with the flow velocity of 80 km/s. Therefore, the velocity difference between the carbon and bulk ions, expected by the neoclassical theory, (2–3 km/s) is small enough to be neglected in this measurement in the LHD. The assumption of equal toroidal flow velocity between the carbon and bulk ions could be invalid in the pedestal region where the ion pressure gradient is large.[25]

D. Effect of the offset of toroidal rotation velocity on the D-H ratio measurements

Since the toroidal rotation velocity measured with carbon charge exchange spectroscopy is used to determine the wavelength shift of the H and D hot components, the uncertainty of the carbon charge exchange spectroscopy measurement has a strong influence on the determination of D-H ratio. As seen in the toroidal ration

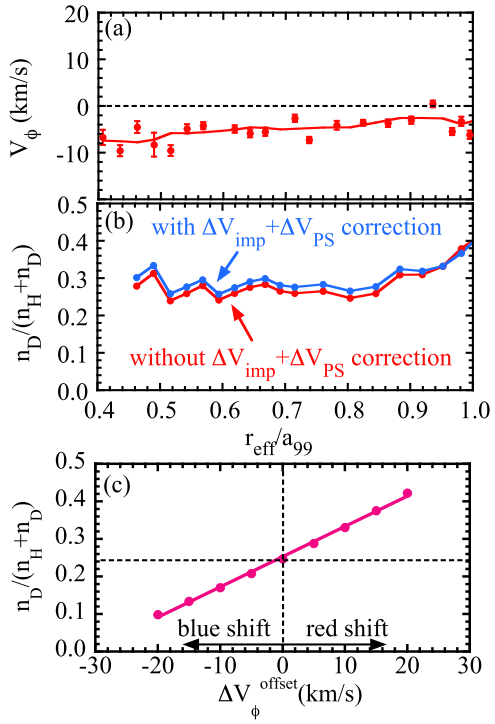

FIG. 7. Radial profile of (a) toroidal rotation velocity and (b) deuterium fraction with and without correction of velocity difference between impurity and bulk ions, and (c) the deuterium fraction as a function of the offset of carbon toroidal rotation velocity.

profiles in Fig. 7(a), the statistical error bar of the toroidal rotation velocity measurements based on the photon noise is relatively small. The largest uncertainty in the absolute value of toroidal rotation velocity is due to the uncertainty of the absolute wavelength calibration of the spectrometer. This uncertainty of the absolute wavelength calibration (typically 0.01 nm) gives the offset of the toroidal rotation velocity of ~5 km/s in velocity. The velocity differences between the carbon and bulk ions discussed in Sec. IV C are only 2–3 km/s, and the influence of the determination of D-H ratio is relatively small, as seen in Fig. 7(b). By including the velocity differences, the D fraction increases only 0.02–0.03. The influence of the offset of the toroidal rotation velocity measured to the determination of the D-H ratio is studied to evaluate the systematic error bar of this measurement. The offset of the toroidal rotation is scanned from −20 km/s (blue shift) to +20 km/s (red shift). The influence is evaluated from the slope of Fig. 7(b) and is 0.008/km/s. The systematic error bar owing to the uncertainty of the offset of the carbon toroidal rotation measurement (5 km/s) is 0.04.

V. HYDROGEN AND DEUTERIUM DENSITY PROFILE IN THE D-H MIXTURE PLASMA WITH PELLET INJECTION

Radial profiles of isotope density are calculated from the intensity of the hot component and integrated beam density along the line of sight. Figure 8 shows the radial profile of intensity of deuterium and hydrogen hot components, line integrated beam density, and density of deuterium and hydrogen. The line integrated beam density is obtained by integrating the local beam density calculated by the beam attenuation code[26] based on the electron temperature and the density profiles measured. The line integrated beam density decreases toward the plasma center by a factor of ~3 due to beam attenuation and beam divergence. In order to derive the deuterium density profile, the effect of halo neutral[27] should be taken into account because the halo contribution can be very large at low temperature and high density.[28] The halo contribution is calculated with FIDAsim[29] using the density and temperature profiles measured. The difference of halo contribution by the interaction with the hydrogen ion and with the deuterium ion is relatively small, as seen in Fig. 8(c). Both the hydrogen and the deuterium density profiles are flat or slightly hollow in the core region, and there are no significant differences in the profiles between hydrogen and deuterium.

In order to confirm the validity of this measurement, the hydrogen and deuterium pellet injection experiment into the D-H mixture plasma was performed in the LHD.[30] Figure 9 shows the time evolution of radial profiles of hydrogen and deuterium density 25 ms

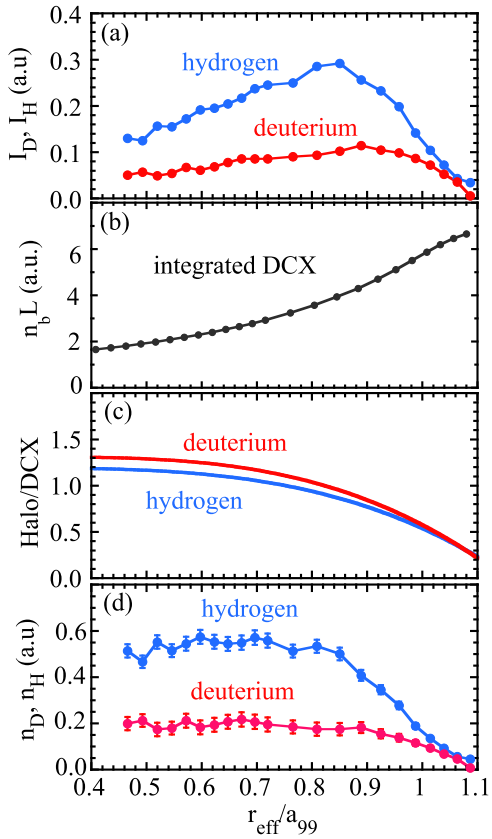

FIG. 8. Radial profile of (a) intensity of deuterium and hydrogen hot components, (b) line integrated beam density, (c) the ratio of Halo contribution to direct change exchange (DCX) contribution, and (d) density of deuterium and hydrogen.

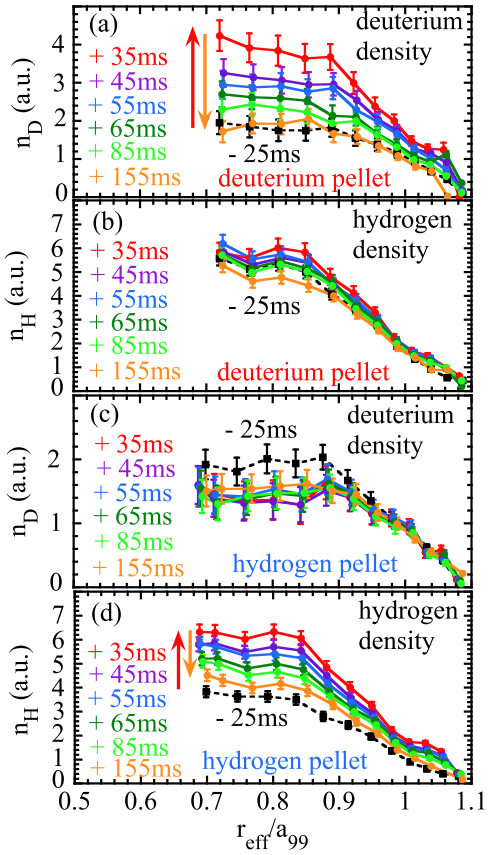

FIG. 9. Radial profile of [(a) and (c)] deuterium and [(b) and (d)] hydrogen density in the plasma with [(a) and (b)] deuterium and [(c) and (d)] hydrogen pellet injection.

before and 35 ms–155 ms after the hydrogen and deuterium pellet injection into the hydrogen and deuterium mixture plasma. These results demonstrate the validity of the isotope density measurements by bulk charge exchange spectroscopy because the densities of the isotope species injected by the pellet are doubled, but the densities of the other isotope species are almost unchanged. Although ablation of the pellet is located near the plasma periphery, significant increases of ion density of the pellet are observed 35 ms after the pellet injection. Hydrogen and deuterium densities each increase by a factor of 2 due to the particle fueling of hydrogen and deuterium pellets, respectively. Then, the deuterium ion density gradually decreases to the level before the deuterium pellet injection. In contrast, hydrogen density decay is saturated at 155 ms after the hydrogen pellet because of the increase of the recycling of hydrogen from the wall.

VI. SUMMARY

A bulk charge exchange spectroscopy system has been applied to measure the radial profiles of hydrogen (H) and deuterium (D) density in the isotope mixture plasma in the Large Helical Device (LHD). The line of sight of the bulk charge exchange is tilted to neutral beam by 60° (90° is perpendicular) toward the upstream of the neutral beam in order to avoid the interference of beam emission to the red wing of the H_α and D_α spectrum. Charge exchange lines of H_α and D_α are fitted by 4 Gaussian of H and D cold components and H and D hot components with 5 parameters. The measurements of plasma toroidal rotation velocity with carbon charge exchange spectroscopy are combined. Five parameters to be fitted are the amplitude of cold and hot components of deuterium and hydrogen, respectively, and the ion temperature of bulk ions (same ion temperature for deuterium and hydrogen ions).

The wavelength shift of the hot component of H_α and D_α is inferred from the toroidal rotation velocity measured with carbon charge exchange spectroscopy. Although the velocity differences between the carbon and bulk ions are found to be small enough to be neglected, the charge exchange cross-sectional effect on the flow measurements is significantly large and should be taken into account using precise atomic data including the fraction of $n = 2$ excited state in the neutral beam which is experimentally determined. The uncertainty of the offset of the carbon toroidal rotation velocity gives a systematic error of 0.04 in the isotope fraction in this measurement. The validity of the hydrogen and deuterium density profiles is confirmed by the hydrogen and deuterium pellet injection in the D-H mixture plasmas in the LHD.

ACKNOWLEDGMENTS

The authors wish to thank the LHD Experiment Group for the excellent support of this work. One of the authors (K.I.) acknowledges Dr. M. Yoshida (National Institutes for Quantum and Radiological Science and Technology; QST) for providing us with two spectrometers for the bulk charge exchange spectroscopy. This work was supported by the National Institute for Fusion Science grant administrative budgets (Nos. NIFS10ULHH021 and NIFS17KLPH030) and JSPS KAKENHI Grant Nos. JP15H02336, JP16H02442, and JP17H01368.

REFERENCES

[1] P. C. Efthimion, L. C. Johnson, J. D. Strachan, E. J. Synakowski, M. Zarnstorff, H. Adler, C. Barnes, R. V. Budny, F. C. Jobes, M. Louglin, D. McCune, D. Mueller, A. T. Ramsey, G. Rewoldt, A. L. Roquemore, W. M. Tang, and G. Taylor, Phys. Rev. Lett. **75**, 85 (1995).
[2] C. Bourdelle, Y. Camenen, J. Citrin, M. Marin, F. J. Casson, F. Koechl, M. Maslov, and JET Contributors, Nucl. Fusion **58**, 076028 (2018).
[3] M. Yoshinuma, K. Ida, M. Yokoyama, M. Osakabe, and K. Nagaoka, Fusion Sci. Technol. **58**, 375 (2010).
[4] S. R. Haskey, B. A. Grierson, K. H. Burrell, C. Chrystal, R. J. Groebner, D. H. Kaplan, N. A. Pablant, and L. Stagner, Rev. Sci. Instrum. **87**, 11E553 (2016).
[5] S. R. Haskey, B. A. Grierson, C. Chrystal, A. Ashourvan, K. H. Burrell, R. J. Groebner, E. A. Belli, L. Stagner, D. J. Battaglia, T. Stoltzfus-Dueck, and A. Bortolon, Plasma Phys. Controlled Fusion **60**, 105001 (2018).
[6] K. Ida, M. Yoshinuma, B. Wieland, M. Goto, Y. Nakamura, M. Kobayashi, I. Murakami, and C. Moon, Rev. Sci. Instrum. **86**, 123514 (2015).
[7] K. Ida, M. Yoshinuma, M. Goto, O. Schmitz, S. Dai, A. Bader, M. Kobayashi, G. Kawamura, C. Moon, Y. Nakamura, and LHD Experiment Group, Plasma Phys. Controlled Fusion **58**, 074010 (2016).
[8] A. Perek, K. Ida, M. Yoshinuma, M. Goto, Y. Nakamura, M. Emoto, R. Jaspers, and LHD Experiment Group, Nucl. Fusion **57**, 076040 (2017).

[9]K. Yamazaki, K. Ida, M. Yoshinuma, and T. Kobayashi, Plasma Fusion Res. **13**, 1202103 (2018).
[10]M. von Hellermannt, P. Bregert, J. Frielingt, R. Konigt, W. Mandls, A. Maast, and H. P. Summers, Plasma Phys. Controlled Fusion **37**, 71 (1995).
[11]M. G. von Hellermann, G. Bertschinger, W. Biel, C. Giroud, R. Jaspers, C. Jupen, O. Marchuk, M. O'Mullane, H. P. Summers, A. Whiteford, and K.-D. Zastrow, Phys. Scr. **T120**, 19 (2005).
[12]K. Fujii, M. Goto, S. Morita, and LHD Experiment Group, Nucl. Fusion **55**, 063029 (2015).
[13]W. M. Solomon, K. H. Burrell, P. Gohil, R. J. Groebner, and L. R. Baylor, Rev. Sci. Instrum. **75**, 3481 (2004).
[14]W. M. Solomon, K. H. Burrell, R. Feder, A. Nagy, P. Gohil, and R. J. Groebner, Rev. Sci. Instrum. **79**, 10F531 (2008).
[15]H. P. Summers, The ADAS user manual version2.6, 2004, www.adas.ac.uk.
[16]J. Chen, K. Ida, M. Yoshinuma, I. Murakami, T. Kobayashi, M. Y. Ye, and B. Lyu, Phys. Lett. A **383**, 1293 (2019).
[17]W. I. vanRij and S. P. Hirshman, Phys. Fluids B **1**, 563 (1989).
[18]D. A. Spong, Phys. Plasmas **12**, 056114 (2005).
[19]H. Sugama and S. Nishimura, Phys. Plasmas **15**, 042502 (2008).
[20]V. V. Nemov, Nucl. Fusion **28**, 1727 (1988).
[21]S. T. A. Kumar, J. N. Talmadge, T. J. Dobbins, F. S. B. Anderson, K. M. Likin, and D. T. Anderson, Nucl. Fusion **57**, 036030 (2017).
[22]H. Sugama and S. Nishimura, Phys. Plasmas **9**, 4637 (2002).
[23]D. A. Spong, J. H. Harris, A. S. Ware, S. P. Hirshman, and L. A. Berry, Nucl. Fusion **47**, 626 (2007).
[24]Y. Yamamoto, *et al.*, "Effect of Pfirsch-Schlüter flow on the inboard/outboard asymmetry of the toroidal flow in LHD," Phys. Plasmas (submitted).
[25]S. R. Haskey, B. A. Grierson, L. Stagner, C. Chrystal, A. Ashourvan, A. Bortolon, M. D. Boyer, K. H. Burrell, C. Collins, R. J. Groebner, D. H. Kaplan, and N. A. Pablant, Rev. Sci. Instrum. **89**, 10D110 (2018).
[26]K. Ida, M. Yoshinuma, T. Kobayashi, Y. Fujiwara, J. Chen, I. Murakami, M. Kisaki, and M. Osakabe, Plasma Fusion Res. **14**, 1402079 (2019).
[27]R. M. McDermott, R. Dux, T. Pütterich, B. Geiger, A. Kappatou, A. Lebschy, C. Bruhn, M. Cavedon, A. Frank, N. den Harder, and E. Viezzer, and ASDEX Upgrade Team, Plasma Phys. Controlled Fusion **60**, 095007 (2018).
[28]B. A. Grierson, K. H. Burrell, C. Chrystal, R. J. Groebner, D. H. Kaplan, W. W. Heidbrink, J. M. Muñoz Burgos, N. A. Pablant, W. M. Solomon, and M. A. Van Zeeland, Rev. Sci. Instrum. **83**, 10D529 (2012).
[29]W. W. Heidbrink *et al.*, Commun. Comput. Phys. **10**, 716 (2011).
[30]K. Ida *et al.*, Nucl. Fusion **59**, 056029 (2019).